
Proceedings Paper:
Dawson, J F, Marvin, A C, Porter, S J et al. (2001) The effect of grounding on radiated emissions from heatsinks. In: IEEE International symposium on EMC, Montreal, 13-17 Aug '01. IEEE International Symposium on Electromagnetic Compatibility, 13-17 Aug 2001 IEEE, MONTREAL, pp. 1248-1252.

https://doi.org/10.1109/ISEMC.2001.950617

The effect of grounding on radiated emissions from heatsinks

J F Dawson, A C Marvin, S J Porter

Department of Electronics
University of York
York, YO10 5DD, England

A Nothofer

National Physical Laboratory
Teddington, TW11 0LW
England

J E Will, S Hopkins

Electromagnetic Compatibility Group
Sun Microsystems Inc.
Palo Alto CA 94303

Abstract: The paper presents results which demonstrate that radiated emissions from heatsinks are reduced by an amount that depends upon the distribution and impedance of the grounding structure. Results are also presented which show the effect on radiated emissions of the presence of conductors (e.g. PCB tracks) passing under the heatsink. The presence of conductors reduces the effectiveness of the heatsink grounding but, in most case, emissions at high frequencies do not exceed those without conductors attached.

Introduction

As operating frequencies of electronic circuits increase into the gigahertz region, components such at heatsinks can become efficient radiators of electromagnetic energy. In order to reduce radiation a heatsink might be grounded. Previous work [1,2,3] has shown that grounding a heatsink can reduce radiated emissions. Here the effect of the impedance and disposition of the grounding structure on radiated emissions is considered. A practical heatsink on a printed circuit board is likely to have tracks which emerge from under the heatsink. The effect of these tracks is also considered.

The majority of the results have been obtained using a full wave numerical electromagnetic simulator (CONCEPT a method of moments solver and Micro−stripes a TLM solver). Validation of the models by measurement has been performed for a number of scenarios.

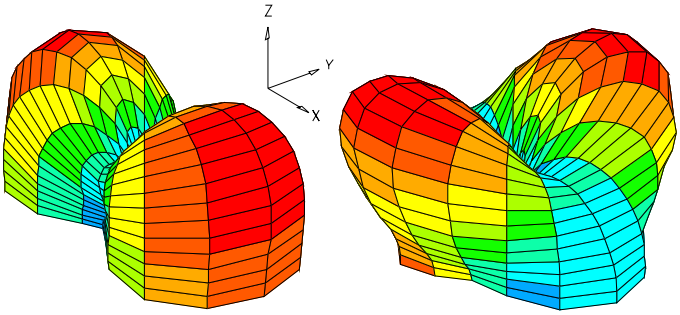

Figure 1: Radiation pattern of the heatsink at 2.5GHz with 24 ground wires (left) and no grounding (right)

We observe in our numerical models that a radiating heatsink can have a complex radiation pattern (Figure 1) so that measurement of the radiated fields at a single point or a small number of points does not give a good picture of the overall radiation or a sensible comparison of the relative emissions of different scenarios. We therefore present results in which the total radiated power is computed. However in order to aid validation of the numerical models we also compute and measure radiated fields received by a monopole antenna 1m from the heatsink.

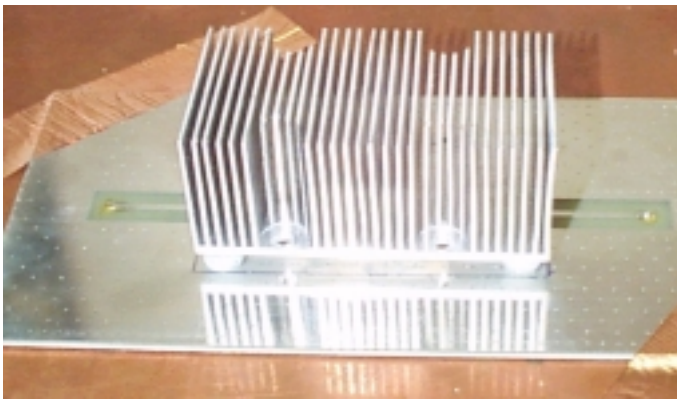

Figure 2: The finned heatsink used as the basis for this paper

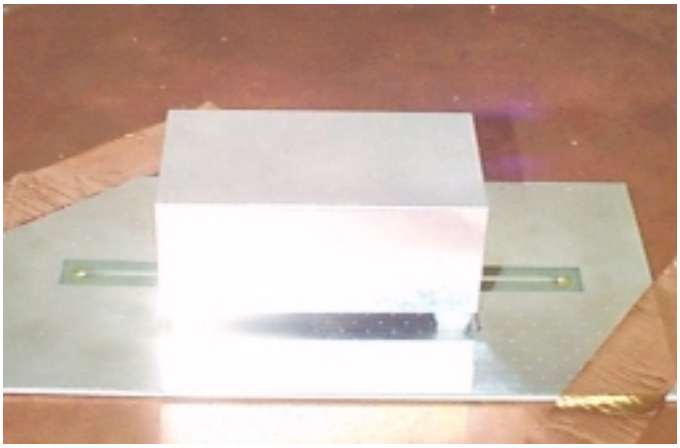

Figure 3: The solid block heatsink used for comparison with the numerical models

We also have observed very little difference in the general electromagnetic behaviour of a finned heatsink and a solid cuboid block. As the solid block allows a much simpler simulation model we have used a solid block in both the measurements and models presented here.

EXPERIMENTAL SETUP

In order to allow validation of the numerical model the setup shown in Figure 4 was used for both measurements and the computational model. The heatsink was supported at each corner by a small dielectric support (not included in the numerical model) over a ground plane. The centre of the heatsink was fed by a 50 Ohm source vi a short wire (0.7 mm diameter) protruding from the ground plane. This is similar to the common mode excitation due to voltage drops in the leads of an IC package and can also be easily produced in the laboratory to allow validation of the model by measurement. A 3cm high monopole at 1 m from the centre of the heatsink, connected to a 50 Ohm load was used to sense the radiated field for model validation purposes.

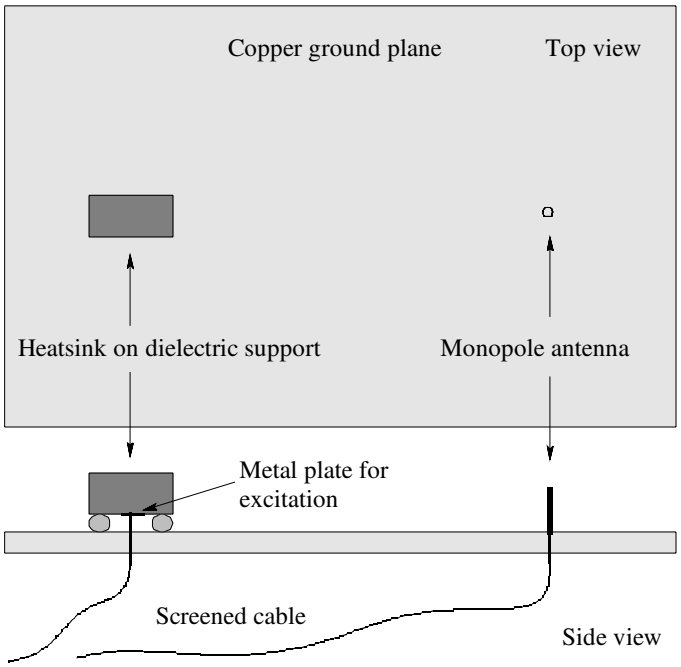

Figure 4: Measurement setup for validation of numerical models

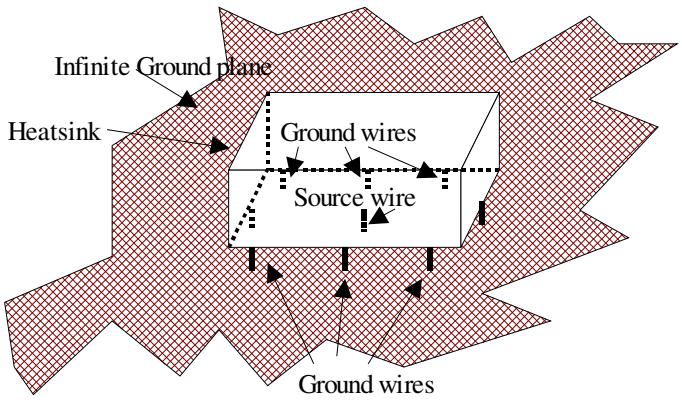

Figure 5: Heatsink over an infinite ground plane with grounding wires (evenly spaced) around periphery.

Figure 5 shows the source and grounding wires distributed evenly around the periphery of the heatsink.

Measurements

Microwave absorber was placed around the edges of the ground plane to limit the effect of reflections from nearby objects, as the measurements were carried out on a laboratory bench.

Measurements were performed using a network analyser to determine the transmission from heatsink to monopole (S21) in order to validate the model.

Numerical modelling

In the CONCEPT (method of moments) numerical model the heatsink was modelled as a cuboid constructed from conducting plates, over an infinite ground plane. The receiving monopole was included in the model so that its load voltage could be directly compared with measurement.

RESULTS

Results for a heatsink 120x50x40mm (LxWxH) in the form of a solid block, 5mm above the ground plane, are presented – other geometries have also been investigated.

Model validation

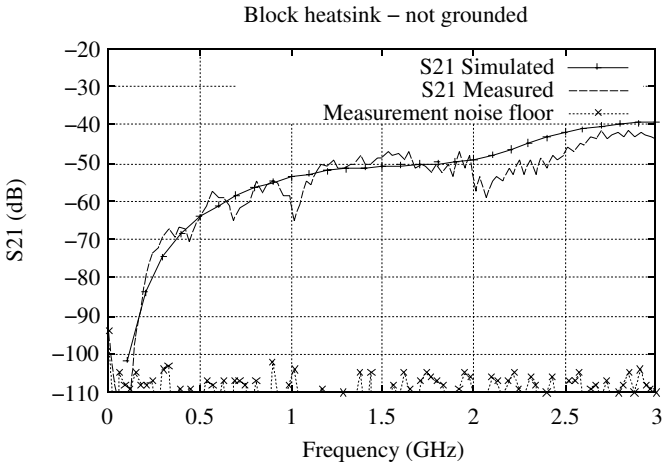

Figure 6: Comparing the measured and simulated S21 from heatsink feed to monopole base for the block heatsink – not grounded.

Figure 6 shows the measured and simulated coupling (S21) from the heatsink to the monopole antenna for the block heatsink with no grounding. Figure 7. compares the simulated and measured S21 when the block heatsink is grounded at each corner with copper tape (real) or a conducting plate (model) – a 5mm wide plate on the short face and a 6mm wide plate on the long face was used at each corner (8– plates).

The small scale detail visible in the measurement results is due to reflections from nearby objects.

Figure 8 shows the ratio of S21 with/without grounding combining the data from Figure 6 and Figure 7. It can be seen that the model predicts the effect of grounding. At

frequencies below 500MHz where the measurement data falls below the noise floor the measured ratio becomes meaningless.

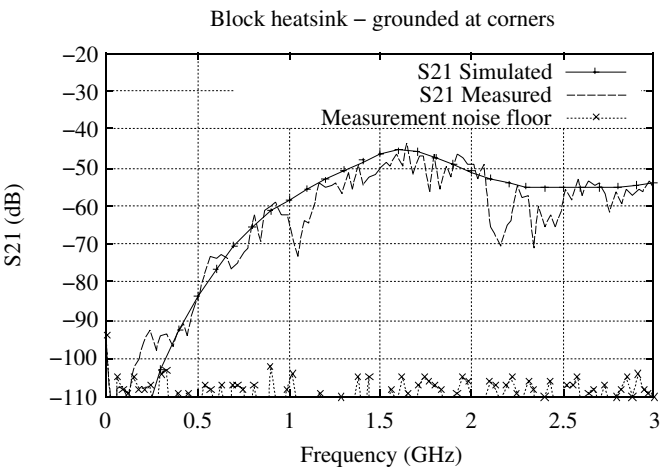

Figure 7: Comparing the measured and simulated S21 from heatsink feed to monopole base for the block heatsink – grounded at each corner with copper tape.

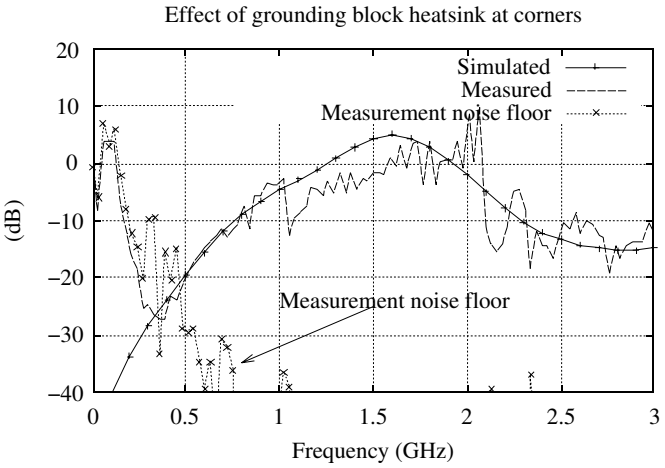

Figure 8: Comparing the measured and simulated effect of grounding grounding just the corners of the block heatsink (Power grounded / Power not grounded).

Effect of grounding on radiated power

Figure 9 shows the effect of different numbers and types of grounding wires on the total radiated power from the heatsink. It can be seen that as the number of grounding wires increases, the radiated power is reduced, and that the frequency at which the grounding ceases to be effective is increased. Also note that in the grounded case the radiated power exceeds the not grounded case over a range of frequencies.

Figure 10 shows the effect of the total inductance of the ground wires on the radiated power. It can be seen that the points on each curve lie approximately in a straight line. The "straight–line" approximation fails beyond the frequency where peak emissions occur.

In terms of the radiated power ratio:

$$\frac{P_g}{P_0} \propto L^m \tag{1}$$

where P_g is the total radiated power in the grounded case and P_0 is the total radiated power in the ungrounded case and L is the total inductance of the grounding conductors acting in parallel. The exponent m depends weakly upon frequency but is approximately 3.5.

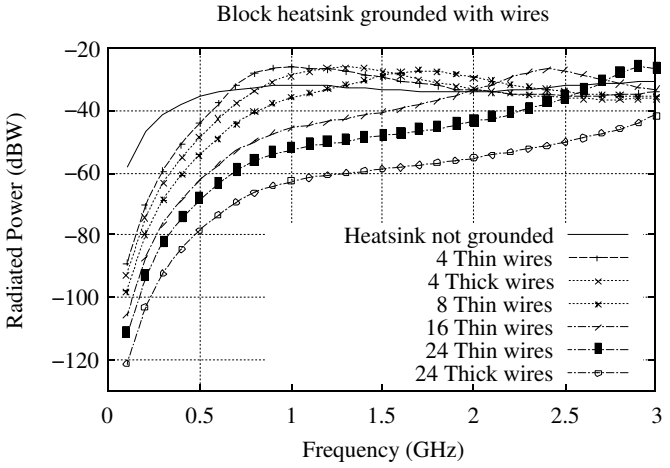

Figure 9: Effect of grounding on the total radiated power of the heatsink (grounded with thin or thick wires).

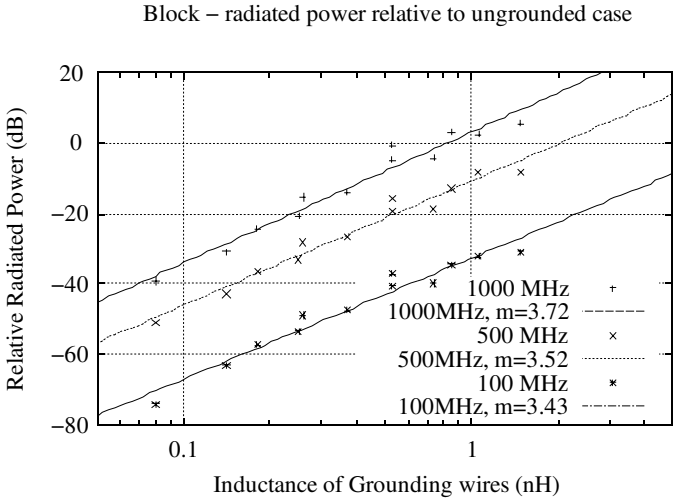

Figure 10: Total radiated power, relative to the ungrounded case, of the grounded heatsink as a function of total inductance of the ground connections for some fixed frequencies, plotted along with the line defined by equation (1) using a least mean squares fit to determine m – wires only

We have also considered the use of plates and square posts for grounding. Figure 11 shows the effect of all of the grounding schemes as a function of their inductance. It can be seen that the "straight–line" relationship is not as clear as

in Figure 10 where only wires were considered.

The self−partial inductance of a wire length l and diameter d is according to [4] (Chapter 6.1.4, p 261)

$$L_{pii} = l\frac{\mu_0}{2\pi}\left[\ln\left(\frac{4l}{d}\right) - 1\right] \quad (1)$$

The self−partial inductance is used as an estimate of the self−inductance of each grounding feature (wire, plate, or post) from its diameter (in case of the wires) or from the diameter which gives the same circumference (in case of the posts). As the plates are modelled with single sided patches (ie they act as a single current sheet, rather than a metal plate with current on both sides), their width is used instead of their circumference. This leads to the following inductance values per grounding feature:

Grounding method	*Inductance in nH*
Thin wire – 0.1 mm dia.	5.9
Thick wire – 0.7 mm dia.	3.4
Plate – 6 mm	2.12
Square post – 5×5 mm	0.56

Table 1: Estimated inductance of each grounding connection.

The total inductance of the grounding can be calculated by dividing the values in Table 1 above by the number of features. This leads to the values given in Table 2 ,which are sorted by increasing inductance.

Inductance in nH	*Grounding method*
0.02	24 posts
0.05	12 posts
0.07	8 posts
0.08	26 plates
0.14	24 thick wires
0.14	4 posts
0.18	12 plates
0.25	24 thin wires
0.26	8 plates
0.28	2 posts
0.37	16 thin wires
0.53	4 plates
0.74	8 thin wires
0.85	4 thick wires
1.06	2 plates
1.48	4 thin wires

Table 2: Estimated inductance of each grounding scheme.

The grounding schemes in Figure 11 that deviate significantly from the "straight−line" approximation are those where a smaller number of posts or plates are used to obtain the same inductance. A given inductance grounding scheme appears to be more effective when a large number of higher inductance ground connections are used, than when a few low inductance connections are used. This is similar to the effect seen in enclosure shielding where a large number of small holes gives better shielding than a smaller number of large holes with the same total area [5].

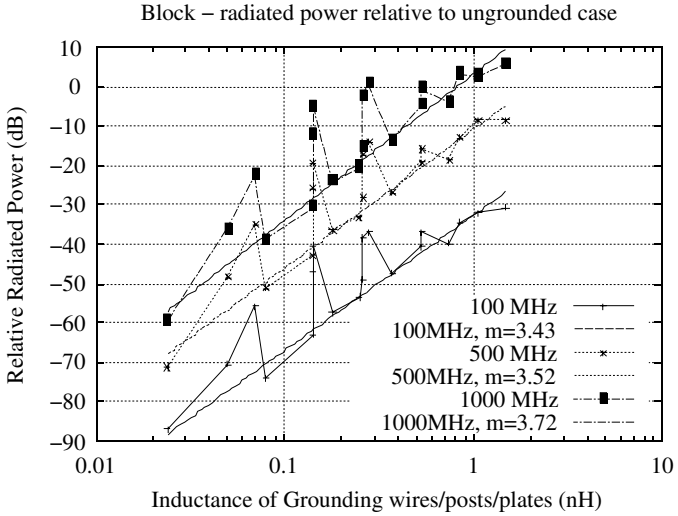

Figure 11: Total radiated power, relative to the ungrounded case, of the grounded heatsink as a function of total inductance of the ground connections for some fixed frequencies, plotted with the line defined by equation (1) using a least mean squares fit to determine m – including posts and plates

Effect of conductors(tracks) on radiated power

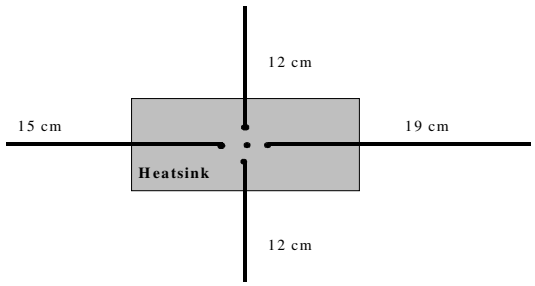

Figure 12: Sketch of the heatsink with horizontal conductors (tracks) underneath, view from below.

Conductors connected to the underside of the heatsink, representing PCB tracks tightly coupled to the heatsink (e.g. via an integrated circuit package) were added to the heatsink as shown in Figure 12. In this case the heatsink was grounded continuously around its periphery, except that four 1cm gaps were made, through which the conductors pass. 3 different lengths were used for the conductors so that the conductor resonances are spread evenly across the spectrum.

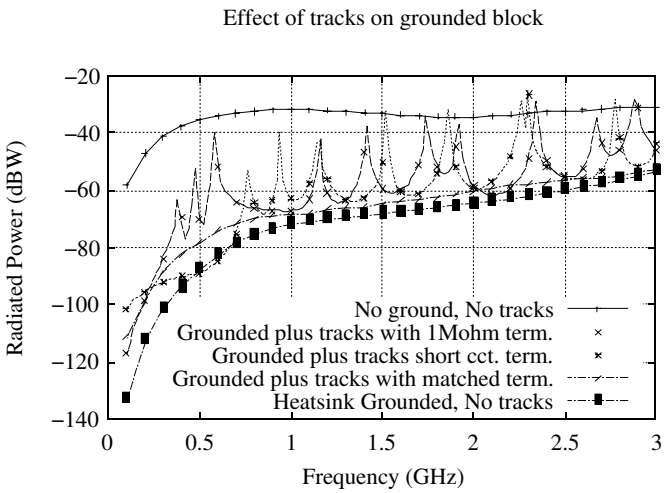

Figure 13: Total radiated power of a well grounded heatsink with and without conductors (tracks) underneath, compared with the case with no conductors and with no grounding.

It can be seen in Figure 13 that the tracks reduce the efficacy of grounding the heatsink and that their effect depends upon their termination. In particular tracks with open or short−circuit termination greatly increase the radiated power at some frequencies. Results for other grounding configurations are similar. For tracks where the terminating impedance is not matched to the track, resonances can cause peaks in emissions which can sometimes exceed the case for the heatsink which is not grounded.

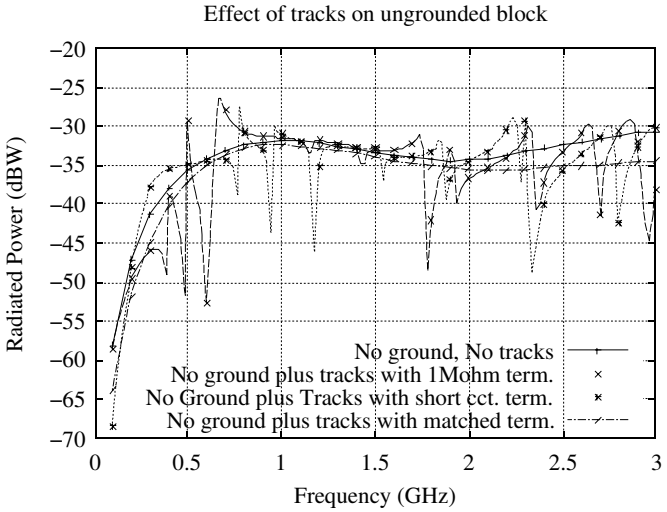

Figure 14: Total radiated power heatsink, not grounded, with and without conductors (tracks) underneath.

It can also be seen in Figure 14 that the presence of short or open−circuit tracks can cause significant narrow−band increases and decreases in the emissions compared with a heatsink that is not grounded.

Conclusions

The efficacy of grounding a heatsink is dependant on the impedance of the ground connections and their distribution. The radiated emissions increase approximately with the inductance of the grounding network to the power of 3.5. We have also observed that an evenly distributed ground structure is up to 20dB better than a poorly distributed scheme of the same overall inductance. The upper frequency limit at which grounding is effective increases with decreasing ground conductor inductance.

The presence of tracks, extending from under the heatsink, limits the effective frequency of grounding but does not make overall radiation significantly worse than the ungrounded case. The presence of tracks connected to the heatsink and grounded with a low impedance can reduce heatsink emissions at low frequencies but also reduces the upper frequency at which the heatsink grounding is effective. Tracks terminated in their characteristic impedance show lower radiation levels than those with short, or open circuit terminations due to damping of track resonances.

Acknowledgement

The authors gratefully acknowledge the support of Sun Microsystems Inc.

References

[1] Kevin Li, Check F. Lee, Soon Y. Poh, Robert T., Shin, and Jin A. Kong. *Application of FDTD method to analysis of electromagnetic radiation from, VLSI heatsink configurations*. IEEE Transactions on Electromagnetic Compatibility, Vol 35, No. 2, May, 1993, pp204–214

[2] N. J. Ryan, D. A. Stone, and B. Chambers. Applica−tion of the FD−TD method to modelling the electro−magnetic radiation from heatsinks. In 10th Interna−tional Conference on Electromagnetic Compatibility, pages 119–124, Warwick, UK, September 1997.

[3] Bruce Archambeault, Satish Pratapneni, and David C. Wittwer. *Comparison of Various Numerical Modelling Tools Against a Standard Problem Concerning Heatsink Emissions,* Presented at IEEE International conference on Electromagnetic Compatibility, Washington, September 2000, available from: www.emcs.org/tc9

[4] Clayton R. Paul. *Introduction to Electromagnetic Compatibility.* Wiley Interscience, 1992, ISBN 0−471−54927−4.

[5] M. P. Robinson, T. M. Benson, C. Christopoulos, J. F. Dawson, M. D. Ganley, A. C. Marvin, S. J. Porter, D. W. P. Thomas, Analytical formulation for the shielding effectiveness of enclosures with apertures, IEEE Trans EMC, Vol 40, No 3, August 1998, pp 240−248